

Global CDNC over
ocean using A-Train
satellites

S. Zeng et al.

This discussion paper is/has been under review for the journal Atmospheric Chemistry and Physics (ACP). Please refer to the corresponding final paper in ACP if available.

Study of cloud droplet number concentration using the A-Train satellites

S. Zeng^{1,2}, J. Riedi³, C. R. Trepte², D. M. Winker², and Y.-X. Hu²

¹Oak Ridge Associated Universities, Oak Ridge, TN, USA

²NASA Langley Research Center, Hampton, Virginia, USA

³Laboratoire Optique d'Atmosphérique, Université Lille 1, Villeneuve d'Ascq, France

Received: 23 September 2013 – Accepted: 28 September 2013

– Published: 7 November 2013

Correspondence to: S. Zeng (shan.zeng@hotmail.com)

Published by Copernicus Publications on behalf of the European Geosciences Union.

Title Page

Abstract

Introduction

Conclusions

References

Tables

Figures

◀

▶

◀

▶

Back

Close

Full Screen / Esc

Printer-friendly Version

Interactive Discussion



Abstract

Cloud droplet number concentration (CDNC) is an important microphysical property of liquid clouds that impacts radiative forcing, precipitation and it is pivotal for understanding of cloud-aerosols interactions. Current studies of this parameter at global scales with satellite observations are still challenging, especially because retrieval algorithms developed for passive sensors (i.e. MODIS/Aqua) have to rely on the assumption of cloud adiabatic growth. The active sensor component of the A-Train constellation (i.e., CALIOP/CALIPSO) allows retrievals of CDNC from depolarization measurements at 532 nm. For that case, the retrieval does not rely on the adiabatic assumption but instead must use a priori information on effective radius (r_e), which can be obtained from other passive sensors.

In this paper, r_e values obtained from MODIS/Aqua and POLDER/PARASOL (two passive sensors, components of the A-Train) are used to constrain CDNC retrievals from CALIOP. Intercomparison of CDNC products retrieved from MODIS and CALIOP sensors is performed, and the impacts of cloud entrainment, drizzling, horizontal heterogeneity, and effective radius are discussed. By analyzing the strengths and weaknesses of different retrieval techniques, this study aims to better understand global CDNC distribution, and eventually determine cloud structure and atmospheric conditions in which they develop. The improved understanding of CDNC should help contribute to future studies of global cloud-aerosol-precipitation interaction and parameterization of clouds in global climate models (GCMs).

1 Introduction

Cloud droplet number concentration is one of the most important cloud microphysical properties as it is intimately related to the cloud droplet size distribution, chemical composition of condensation nucleation nuclei (CCN), and the thermodynamical and dynamical state (i.e., updraft velocity, mixing rates) of the cloudy air during its formation

ACPD

13, 29035–29058, 2013

Global CDNC over ocean using A-Train satellites

S. Zeng et al.

Title Page

Abstract

Introduction

Conclusions

References

Tables

Figures

◀

▶

◀

▶

Back

Close

Full Screen / Esc

Printer-friendly Version

Interactive Discussion



(Seinfeld and Pandis, 1998). This property is directly linked to cloud evolution (i.e. water vapor condensation, droplet nucleation, and drizzling processes). CDNC impacts cloud radiative properties, precipitation development, and it is pivotal in cloud-aerosols interactions, and, thus, influences local/global climate and our daily weather. Many studies have identified that aerosol-cloud interactions constitute the largest source of uncertainties in estimating radiative forcing of the Earth-atmosphere system (Penner et al., 2011). Increasing the number concentration of precursor aerosols may lead to a decrease in cloud effective radius and, therefore, to an increase in cloud albedo (i.e., the first aerosol indirect effect; Twomey, 1977). Recent research shows that in a pristine oceanic atmosphere, the marine biosphere plays a non-negligible role in regulating cloud microphysical properties, and so far many studies have examined biogenic influence on cloud microphysics (Charlson et al., 1987; Lana et al., 2012). Validation of relationships between cloud microphysics and marine biogenic aerosols that serve as CCN can improve our understanding of the ocean-atmosphere interaction. However, studying CDNC at global scales is difficult. While satellites provide broad sampling coverage of continuous observations, retrieval algorithms from passive sensors (e.g., MODIS/Aqua) can suffer from important uncertainties because they rely heavily on assumptions regarding adiabatic or subadiabatic cloud growth. As a matter of fact, most clouds in the atmosphere do not grow adiabatically. Real clouds are predominantly subadiabatic because of warm rain process and droplet evaporation/breakup processes associated to the cloud top entrainment (Pruppacher and Lee, 1976). It is therefore highly relevant to investigate and understand the retrieval bias due to cloud diabatic growth. The active sensor CALIOP/CALIPSO, another A-Train member, permits retrievals of CDNC from the depolarization measurement at 532 nm. This technique differs and has a weak dependence upon an adiabatic assumption. On the other hand, the CDNC retrieval methodology requires a priori information on the r_e , which cannot be derived from CALIOP. This information is retrieved independently from other sensors, such as MODIS/Aqua or POLDER/PARASOL. The CDNC retrieval accuracy, therefore, strongly depends on the accuracy of r_e retrieved from other sensors. This calls for

Global CDNC over ocean using A-Train satellites

S. Zeng et al.

[Title Page](#)[Abstract](#)[Introduction](#)[Conclusions](#)[References](#)[Tables](#)[Figures](#)[◀](#)[▶](#)[◀](#)[▶](#)[Back](#)[Close](#)[Full Screen / Esc](#)[Printer-friendly Version](#)[Interactive Discussion](#)

a careful evaluation and intercomparison of CDNC datasets derived at a global scale from passive (MODIS) and active (CALIOP) sensors based on these different retrieval techniques.

In Sect. 2, the CALIOP/CALIPSO, MODIS/Aqua and POLDER3/PARASOL data are presented, and algorithms, theoretical basis, and main characteristics are summarized. Comparison methodology of CDNC between CALIOP and MODIS and the corresponding results are given in Sect. 3. Impacts of cloud entrainment/drizzling, horizontal heterogeneity, and r_e are discussed in Sect. 4, and conclusions are drawn in Sect. 5.

2 Data and algorithms

In our study, collocated data from official level 2 CALIOP/CALIPSO, MODIS/Aqua and POLDER3/PARASOL products extracted along the CALIOP track (CALTRACK data from ICARE Data and Service Centre, Zeng, 2011) are being considered for the period from November 2007 to December 2008. We provide hereafter a brief summary of the CDNC products used and the algorithm theoretical basis used for their retrievals.

2.1 CALIOP/CALIPSO

CALIOP uses layer integrated depolarization ratio (δ) and droplet effective radius (r_e) to retrieve the CDNC (N , unit: cm^{-3} , see Eq. 1). It is based on the fact that extinction coefficients of water clouds are related to δ (depolarization is related to multiple scatter) and r_e (droplet size determines the proportion of backward/forward scatter) (Hu et al., 2007). The total extinction is a sum of extinction of each single droplet. The main advantage of the method is that adiabatic assumption is not required for the retrieval. The CDNC can be accurately retrieved if layer integrated depolarization ratio and r_e are accurate. However, because the retrieval sensitivity of r_e from the CALIOP extinction and layer integrated depolarization ratio is very low, there is no r_e product derived from CALIOP. Coincident POLDER (Bréon and Doutriaux-Boucher, 2005) or MODIS

Title Page

Abstract

Introduction

Conclusions

References

Tables

Figures

◀

▶

◀

▶

Back

Close

Full Screen / Esc

Printer-friendly Version

Interactive Discussion



r_e retrieved values (Nakajima and King, 1990; Platnick et al., 2003) are used to better constraint the CDNC retrieval. Therefore the retrieval accuracy depends strongly on the correctness of r_e derived from passive instruments.

$$N \approx 1000 \frac{[1 + 135\delta^2/(1 - \delta)^2]}{2\pi(R_e/(1 \mu\text{m}))_{\text{opt}}^5} \quad (1)$$

2.2 MODIS/Aqua

Inference of CDNC from MODIS uses both cloud optical thickness and droplet effective radius, which are obtained directly from a bispectral technique using bi-directional solar visible reflectance and near infrared absorption (Nakajima and King, 1990). Equation (2) is valid under the assumption that clouds develop in adiabatic conditions, implying that liquid water content (the sum of single water droplet mass) increases linearly with height above cloud base (Borg and Benartz, 2007). Results of deviations from this hypothesis have been investigated through comparison to the in-situ observations (Painemal and Zuidema, 2011; Min et al., 2012). The MODIS CDNC values (derived with $f_{\text{ad}} = 0.8$) are quite close to in-situ observations for stratocumulus over the Chile–Peru coast.

$$N_{\text{ad}} = f_{\text{ad}} \frac{\sqrt{10}}{4\pi} \left[\frac{C_w \tau}{\rho_w R_e^5} \right]^{0.5} \quad (2)$$

Above, CDNC (N , unit: cm^{-3}) is a function of cloud optical thickness (τ) and effective radius (r_e). ρ_w is water density. C_w is adiabatic lapse rate, which is an experimental function (Rao et al., 2008) of temperature (obtained from MODIS) and pressure (obtained from CALIOP). f_{ad} is the degree of adiabaticity and in range of $0 < f_{\text{ad}} < 1$. It is assumed a constant value of 1 in our calculation, corresponding to adiabatic. k is the ratio of effective radius to volume radius and is assumed constant at 0.6438 in our for-

Title Page

Abstract

Introduction

Conclusions

References

Tables

Figures

◀

▶

◀

▶

Back

Close

Full Screen / Esc

Printer-friendly Version

Interactive Discussion



mula ($k = 1/((1 - \nu) \times (1 - 2 \times \nu))$); ν is the effective variance of size distribution, $\nu = 0.13$ for MODIS; Hu. et al., 2007).

2.3 POLDER3/PARASOL

Droplet effective radius derived from MODIS tends to be larger than the true value, mostly because of neglecting horizontal photon transport (the 3-D radiative bias) within heterogeneous clouds (Zhang and Platnick, 2011). In addition to the MODIS r_e , we also investigated CDNC retrievals using product of r_e derived from POLDER3/PARASOL. From POLDER observations, r_e can be retrieved using angular polarization signal (Bréon and Doutriaux-Boucher, 2005), which also allows one to determine the size distribution effective variance under specific conditions (narrow size distribution). Although these retrievals are expected to be less susceptible to 3-D radiative biases (Bréon and Doutriaux-Boucher, 2005), they require rather homogeneous cloud fields because of the high angular sampling necessary to analyze the polarization backscatter features. These retrievals are therefore performed and products provided at a much coarser resolution than their MODIS counterparts. However, because they are derived from polarization measurements, the retrievals are very sensitive to particle size at the very top of clouds, which makes them relevant for use in combination with CALIOP measurements.

3 Results

MODIS allows to use three bands in the near infrared (at $1.6 \mu\text{m}$, $2.1 \mu\text{m}$ and $3.7 \mu\text{m}$ bands) to retrieve r_e . The retrieval is based on absorption in these bands that provides sensitivity to r_e (Nakajima and King, 1990). In our study, we used the MODIS $3.7 \mu\text{m}$ effective radius ($r_{e,3.7}$) retrieval only to calculate both MODIS and CALIOP CDNCs. This is because the $r_{e,3.7}$ is expected to be the closest to the cloud top (Platnick, 2000) and the least sensitive to the 3-D radiative bias (Zhang and Platnick, 2011), and is

therefore what we need for our calculation. In this section, we will show geographical distributions, seasonal variations, and the observed relationship between CALIOP and the MODIS CDNCs. Discussions about different factors impacting the CDNC retrieval are provided in the next section.

5 3.1 Geographical distributions of CDNC and their differences

In Fig. 1, we present geographical distributions of the CDNC derived from MODIS (a) and CALIOP (b) and their relative differences calculated as the ratio of CDNC differences (CALIOP-MODIS) to the mean CDNC of the two sensors. In general, we see that the two sensors show similar geographical distributions of CDNC with MODIS values globally larger than CALIOP ones (bar scales are different). Higher droplet number concentrations are found around continents and in the Storm Tracks, which agree with model simulations and observations of aerosols (Barahona et al., 2011; Moore et al., 2009, 2013; Vignati et al., 2011; Remer et al., 2008). However, over the open ocean, values are as low as fewer than 100 cm^{-3} for both sensors. Relative differences are smaller in those regions where homogenous clouds and adiabatic conditions are known to occur, i.e. off the western coasts of continents and in the subsidence regimes of Storm Tracks.

3.2 Seasonal variations of CDNC

In Fig. 1, we have illustrated that MODIS and CALIOP CDNCs have similar geographical distributions. We also investigate whether they have similar seasonal variations. Figure 2 presents the geographical distributions of the correlation coefficients (a) and the slopes (b) between monthly MODIS and CALIOP CDNCs, and seasonal variations of MODIS (dashed line) and CALIOP (solid line) CDNCs for four specific regions. The correlation coefficients and the slopes are calculated from linear relationships (the CALIOP CDNC as a function of the MODIS one) of monthly mean CDNCs of MODIS and CALIOP (12 months counted). Seasonal variation is represented as the ratio of differ-

Global CDNC over ocean using A-Train satellites

S. Zeng et al.

Title Page

Abstract

Introduction

Conclusions

References

Tables

Figures



Back

Close

Full Screen / Esc

Printer-friendly Version

Interactive Discussion



Global CDNC over ocean using A-Train satellites

S. Zeng et al.

Title Page

Abstract

Introduction

Conclusions

References

Tables

Figures

◀

▶

◀

▶

Back

Close

Full Screen / Esc

Printer-friendly Version

Interactive Discussion



ences between monthly and annual mean values to the annual mean value. In Fig. 2a, we see that MODIS and CALIOP CDNCs have similar seasonal variations over the whole globe with correlation coefficients superior to 0.5, in particular for the regions to the west of continents where correlation coefficients are as high as more than 0.9. In Fig. 2b, we see the slopes are as high as about 0.6 in the regions to the west of continents, which means the CALIOP CDNC is about 0.6 of the MODIS one, but values are quite low in the other regions. Seasonal cycles of CDNC show similar trends between CALIOP and MODIS for different regions (Fig. 2c–f) though they differ from region to region: CDNCs are higher in winter and lower in summer to the east of China; CDNCs are higher in spring and autumn and lower in winter to the west of California; CDNCs are higher in January, May and September to the west of Peru; and CDNCs are higher in April and July to the west of Namibia. The underline reasons for CDNC seasonal variations will be studied in a future research that are related to seasonal changes of different CCN sources. However it is out of the objective of this paper and thus will not be discussed here.

3.3 Relationship between MODIS and CALIOP CDNC

In Fig. 3, we present the two-dimensional relationship between the MODIS and the CALIOP CDNCs. From this figure, we clearly see that CALIOP and MODIS CDNCs are strongly correlated with a correlation coefficient as high as 0.8. The CALIOP CDNC is on average about two third (0.64) of the MODIS one. It supports relationships shown in Figs. 1 and 2, which indicate, despite using very different techniques for the retrievals, that CDNCs derived from the two sensors are quite similar with the MODIS values larger than the CALIOP ones. Although it is still hard to determine at this stage which sensor represents the most accurate CDNC values, their spatial and seasonal distributions can at least be observed consistently from both datasets. This allows us to quantitatively determine regions of highest CDNC compared to others.

4 Discussions

As was mentioned in Sect. 2, the accuracy of CDNC retrieval depends on the accuracy of derived r_e for CALIOP and on the adiabaticity degree of the atmosphere for MODIS. In this section, we discuss possible impacts.

4.1 Impact of cloud entrainment and drizzling

Real clouds in the atmosphere are predominantly subadiabatic for at least two reasons. First, cloud top entrainment induces dry air to mix in clouds and produces a decrease of r_e and CDNC due to evaporation. Second, warm rain processes, such as drizzling, produce a decrease of r_e and CDNC at the cloud top. As was mentioned in Sect. 2, the subadiabaticity can impact the retrieval of the MODIS CDNC via the degree of adiabaticity f_{ad} , and the real value should be smaller than retrieval because f_{ad} is always inferior to unit.

As cloud adiabaticity has an impact on both r_e and CDNC and biases the values at cloud top towards the same direction, in Fig. 4a, we present geographical distribution of relative differences of r_e between the 3.7 μm ($r_{e,3.7}$) and the 2.1 μm ($r_{e,2.1}$) bands from MODIS (relative differences are the ratio of r_e differences to r_e mean values). In theory, $r_{e,3.7}$ corresponds to effective radius closer to the cloud top compared to $r_{e,2.1}$ (Platnick, 2000; Zhang and Platnick, 2011), and its value should be larger than $r_{e,2.1}$ according to classic adiabatic growth model (Brenguier et al., 2000). From Fig. 4a, we find in some well-known adiabatic and homogeneous cloud regions (i.e., in the Storm Tracks and to the west of continents), differences of $r_{e,3.7}$ and $r_{e,2.1}$ are close to zero or slightly positive, while in other places differences are negative. Comparing Figs. 4a to 1c, it is clear that CDNC differences and r_e differences between 2.1 μm and 3.7 μm bands show similar geographic distributions. In the Storm Tracks and to the west of continents, both differences are small partially due to less subadiabatic bias (f_{ad} close to 1). For subadiabatic conditions in the other regions, MODIS CDNC retrieval calculated with adiabatic assumption is larger than the real value because

Title Page

Abstract

Introduction

Conclusions

References

Tables

Figures

◀

▶

◀

▶

Back

Close

Full Screen / Esc

Printer-friendly Version

Interactive Discussion



Global CDNC over ocean using A-Train satellites

S. Zeng et al.

Title Page

Abstract

Introduction

Conclusions

References

Tables

Figures

◀

▶

◀

▶

Back

Close

Full Screen / Esc

Printer-friendly Version

Interactive Discussion



the real value is equal to the retrieval value from adiabatic assumption multiplied the degree of adiabaticity f_{ad} (where $0 < f_{ad} < 1$). But for CALIOP, CDNC retrieval does not depend on adiabatic assumption. The differences between CALIOP and MODIS to a certain extent can indicate the degree of adiabaticity: larger differences appear when subadiabaticity tends to be important, while smaller differences appear when in adiabatic conditions.

In Fig. 4b, we show the two-dimensional histogram of the pixel number as a function of the CDNC differences, and the r_e differences between 3.7 μm and 2.1 μm bands. From this later figure, we see that most of the CDNC differences decrease when r_e differences decrease. The correlation coefficient of the linear relationship is 0.53. This means that the more important the subadiabaticity is, the larger are the negative differences between $r_{e, 3.7}$ and $r_{e,2.1}$, and the larger are the negative differences between CALIOP and MODIS CDNCs (f_{ad} is smaller). The CALIOP and MODIS CDNCs are quasi-equal when $r_{e,3.7}$ is much larger than $r_{e,2.1}$, most likely corresponding to cases of adiabatic conditions.

For further verification of adiabatic effect on the CDNC retrieval, in particular for cases of drizzling, we plot in Fig. 5 the two dimensional histograms of relative CDNC difference against $r_{e,2.1}$ (a) and relative r_e difference ($r_{e,3.7} - r_{e,2.1}$) against $r_{e,2.1}$ (b). The histogram is normalized for each r_e bin. According to Nakajima et al. (2010a and 2010b) with collocated CloudSat observations, clouds with MODIS $r_{e,2.1} > 15$ are often found to be associated to drizzle. From Fig. 5, we see both relative CDNC differences and relative r_e differences are important when $r_{e,2.1}$ is superior to 15. This suggests that increasing differences between $r_{e,2.1}$ and $r_{e,3.7}$ and between MODIS and CALIOP CDNCs with r_e is a result of increasing drizzle probability with increasing $r_{e,2.1}$. Drizzling effect on CDNC differences between CALIOP and MODIS (about 0.3 of bias) is larger than on r_e differences between $r_{e,3.7}$ and $r_{e,2.1}$ (about 0.2 of bias).

4.2 Impact of horizontal heterogeneity and 3-D radiative effect

A recent study from Zhang and Platnick (2011) has demonstrated the $r_{e,3.7}$ and $r_{e,2.1}$ differences are not only a result of cloud entrainment and drizzling, but also to a large extent, attributed to the horizontal photon transport, namely the 3-D radiative bias caused by the plan parallel cloud assumption in the retrieval (Zhang and Platnick, 2011; Di Girolamo, 2013). Cloud heterogeneity has a more important impact on the retrieval of $r_{e,2.1}$ than on the $r_{e,3.7}$. It has been found that r_e derived from MODIS is slightly larger than the in-situ measurements (Painemal and Zuidema, 2011). Compared to the 3-D radiative transfer models, r_e bias is about 4–6 μm over the globe with different biases for different clouds, i.e. 1–2 μm for less heterogeneous marine Stratiform clouds, 7–12 μm for more heterogeneous marine cumuliform clouds (Di Girolamo, 2013). This cloud horizontal heterogeneity can impact the CDNC retrievals mainly via the uncertainty on r_e and τ retrieval.

In Fig. 6, we plot the two dimensional histograms between relative CDNC differences and cloud heterogeneity (a) and between relative r_e differences ($r_{e,3.7} - r_{e,2.1}$) and cloud heterogeneity (b). The color bar represents normalized pixel number to each bin of cloud heterogeneity, which is represented by the ratio of the standard deviation to the mean COT derived from MODIS level 2 products into a 20 km \times 20 km grid box. The r_e differences slightly decrease with cloud heterogeneity (Fig. 6b), while the CDNC differences decrease more significantly when clouds become inhomogeneous (Fig. 6a). When clouds become inhomogeneous, retrieved r_e using 1-D radiative transfer model is larger than the true value (Di Girolamo, 2013). According to Eqs. (1) and (2), CDNC is a $-5/3$ power function of r_e for CALIOP and $-5/2$ power function of r_e for MODIS. Therefore compared to MODIS, the CALIOP derived CDNC is smaller than the true value when r_e bias increases, resulting in a negative CDNC bias that increases towards inhomogeneous clouds.

[Title Page](#)[Abstract](#)[Introduction](#)[Conclusions](#)[References](#)[Tables](#)[Figures](#)[◀](#)[▶](#)[◀](#)[▶](#)[Back](#)[Close](#)[Full Screen / Esc](#)[Printer-friendly Version](#)[Interactive Discussion](#)

4.3 Impact of effective radius

The selection of r_e is quite important for retrievals of CDNC from CALIOP. Derivation of r_e from satellite observations is subject to numerous uncertainties. For example, in-cloud vertical structure and drizzle, horizontal cloud heterogeneity, droplet size distribution, cloud fraction, surface reflectance, aerosol, etc., can impact the retrieval accuracy (Zhang and Platnick, 2011; Breon and Doutriaux-Boucher, 2005). Retrieval of r_e from MODIS is based on shortwave infrared band absorption (Nakajima and King, 1990), and its value is found slightly larger than in-situ observations (Min et al., 2012; Painemal and Zuidema, 2011). POLDER uses a different method to retrieve r_e , based on angular polarization signal near cloudbow directions (Breon and Doutriaux-Boucher, 2005). The angular position of maxima and minima in the polarized phase function is only sensitive to r_e and expected to be less biased by 3-D radiative effects. However, this method is applicable only for clouds with narrow size distributions, which are required to produce significant polarization supernumerary bows on which the technique relies. Also due to the angular sampling required to analyze the polarized phase function, the POLDER retrievals currently available are significantly coarser (200 km \times 200 km) than the MODIS ones. These two factors, namely the high sensitivity to narrow size distribution and the large area required to perform retrievals, can potentially also bias r_e retrieved from POLDER in a way that might have been underestimated before. In practice, for large areas within which cloud optical thickness varies significantly, the average polarization signal will be an average of the polarized reflectance produced at smaller scales. Because polarized reflectance gets saturated rapidly compared to total radiance, the resulting polarization signal is not a radiative weighted average of individual contribution but a simple mean. Therefore, thin clouds that tend to contribute less signal in total radiance measurements, do weight equally with thicker clouds when it comes to polarization reflectance. In conclusion, although at rather small scales it is true that polarization is less subject to 3-D effects than total radiance, it remains that using polarized reflectance averaged over large areas can induce some non-intuitive

Title Page

Abstract

Introduction

Conclusions

References

Tables

Figures



Back

Close

Full Screen / Esc

Printer-friendly Version

Interactive Discussion



Global CDNC over ocean using A-Train satellites

S. Zeng et al.

Title Page

Abstract

Introduction

Conclusions

References

Tables

Figures

◀

▶

◀

▶

Back

Close

Full Screen / Esc

Printer-friendly Version

Interactive Discussion



biases. As a simple example, if we assume that thinner parts of a cloud field have smaller r_e than thicker parts, then the r_e retrieved from polarization might be biased low compared to r_e retrieved from a bi-spectral technique which is inferred from total radiance and corresponds to an r_e which, to a first order, is more weighted by total cloud water content. This type of bias could be even more important in case of correlation between cloud optical thickness and droplet size distribution width to which the polarization technique is very sensitive. Until higher resolution polarization measurements or retrievals can be obtained, the POLDER r_e retrievals shall not be considered free of potential biases and the above considerations shall be kept in mind when trying to draw conclusions from the comparison of POLDER and MODIS r_e and derived CDNC values. With that in mind the POLDER r_e are found smaller than the MODIS ones which calls for further understanding of these differences as the selection of r_e is quite critical for the accuracy of CDNC retrieved from CALIOP.

In Fig. 7, we show the geographical distributions of CALIOP CDNC obtained by using MODIS $r_{e,3.7}$ (a), POLDER r_e (b), and relative differences between using MODIS $r_{e,3.7}$ and POLDER r_e (c). Because the POLDER r_e is smaller than the MODIS one and the CDNC is a $-5/3$ power function of r_e (Eq. 2), the CDNC calculated using the POLDER r_e are much higher than when using the MODIS $r_{e,3.7}$. The CDNC can reach to about 600 cm^{-3} to the west of continents using the POLDER r_e , while the values are on the order of about 150 cm^{-3} using the MODIS $r_{e,3.7}$. Over the open oceans, the CDNC values are on the order of about 200 cm^{-3} using the POLDER r_e and about 50 cm^{-3} using the MODIS $r_{e,3.7}$. It illustrates again that using different r_e , results in quite different CDNC values retrieved from CALIOP: using MODIS r_e CDNCs are slightly lower than the values used in GCMs, while using POLDER r_e , these are higher than the GCM results (Barahona et al., 2011). It may suggest the POLDER r_e is quite close to the cloud top and may be a lot affected by the aerosols and dry air, or less impact by 3-D radiative effect, which results in a smaller retrieved r_e value corresponding to a level above the saturated level of the CALIOP backscatter signal.

5 Conclusions

Cloud droplet number concentration is one of the most important key parameters of cloud microphysics. In this paper we examined their geographical distributions and seasonal variations with the MODIS and CALIOP observations. Although these two sensors use quite different techniques to retrieve CDNC, they show similar geographical distributions and seasonal variations. The CALIOP CDNCs are globally smaller than the corresponding MODIS retrievals, being about 0.64 of the MODIS values. The correlation between the two is as high as 0.8. We discussed the possible differences from impacts of cloud entrainment/drizzling, heterogeneity/3-D radiative effect, and r_e used. As the degree of adiabaticity increases, $r_{e,3.7}$ is smaller than $r_{e,2.1}$, and the MODIS retrieved CDNC is larger than the CALIOP one. As cloud heterogeneity increases, retrieved CDNC differences become important between CALIOP and MODIS. CALIOP has advantages in calculating CDNC in subadiabatic systems but its accuracy is highly controlled by the accuracy of the r_e assumption used in the algorithm. Using POLDER effective r_e , retrieved CDNCs are much larger than using MODIS $r_{e,3.7}$. More accurate CDNC values from CALIOP allow, in combination with MODIS, to study important cloud processes such as cloud entrainment. This calls for the development of better r_e retrievals and improved description of r_e vertical profiles. This preliminary work finally open perspective for the future study of the cloud-aerosol interaction, especially the marine biogenic aerosol impacts on cloud microphysics.

Acknowledgements. The authors are very grateful to NASA Langley and Goddard Centers and the French ICARE Data and Services Center for providing the CALIOP, POLDER and MODIS data used in this study. This research has been supported by NASA Postdoc Program.

Global CDNC over ocean using A-Train satellites

S. Zeng et al.

Title Page

Abstract

Introduction

Conclusions

References

Tables

Figures



Back

Close

Full Screen / Esc

Printer-friendly Version

Interactive Discussion



References

- Barahona, D., Sotiropoulou, R., and Nenes, A.: Global distribution of cloud droplet number concentration, autoconversion rate, and aerosol indirect effect under diabatic droplet activation, *J. Geophys. Res.*, 116, D09203, doi:10.1029/2010JD015274, 2011.
- 5 Borg, L. A. and Benartz, R.: Vertical structure of stratiform marine boundary layer clouds and its impact on cloud albedo, *Geophys. Res. Lett.*, 34, 5, doi:10.1029/2006GL028713, 2007.
- Bréon, F.-M. and Doutriaux-Boucher, M.: A comparison of cloud droplet radii measured from space, *IEEE T. Geosci. Remote*, 43, 1796–1805, 2005.
- Brenguier, J.-L., Pawlowska, H., Schüller, L., Preusker, R., Fischer, J., and Fouquart, Y.: Radiative properties of boundary layer clouds: Droplet effective radius versus number concentration, *J. Atmos. Sci.*, 57, 803–821, 2000.
- 10 Charlson, R. J., Lovelock, J. E., Andreae, M. O., and Warren, S. G.: Oceanic phytoplankton, atmospheric sulfur, cloud albedo and climate, *Nature*, 326, 655–661, 1987.
- Di Girolamo, L.: Confronting spatial heterogeneity in passive satellite remote sensing of cloud and aerosol properties, presented at GRC, New London, NH, USA, June, 7–12, 2013.
- 15 Lana, A., Simó, R., Vallina, S. M., and Dachs, J.: Potential for a biogenic influence on cloud microphysics over the ocean: a correlation study with satellite-derived data, *Atmos. Chem. Phys.*, 12, 7977–7993, doi:10.5194/acp-12-7977-2012, 2012.
- Min, Q., Joseph, E., Lin, Y., Min, L., Yin, B., Daum, P. H., Kleinman, L. I., Wang, J., and Lee, Y.-N.: Comparison of MODIS cloud microphysical properties with in-situ measurements over the Southeast Pacific, *Atmos. Chem. Phys.*, 12, 11261–11273, doi:10.5194/acp-12-11261-2012, 2012.
- 20 Moore, R. H., Karydis, V. A., Capps, S. L., Latham, T. L., and Nenes, A.: Droplet number uncertainties associated with CCN: an assessment using observations and a global model adjoint, *Atmos. Chem. Phys.*, 13, 4235–4251, doi:10.5194/acp-13-4235-2013, 2013.
- 25 Moore, T. S., Campbell, J. W., and Dowell, M. D.: A class-based approach to characterizing and mapping the uncertainty of the MODIS ocean chlorophyll product, *Remote Sens. Environ.*, 113, 2424–2430, 2009.
- 30 Nakajima, T. and King, M. D.: Determination of the optical thickness and effective radius of clouds from reflected solar radiation measurement. Part I: Theory, *J. Atmos. Sci.*, 47, 1878–1893, 1990.

Title Page

Abstract

Introduction

Conclusions

References

Tables

Figures

◀

▶

◀

▶

Back

Close

Full Screen / Esc

Printer-friendly Version

Interactive Discussion



Global CDNC over ocean using A-Train satellites

S. Zeng et al.

Title Page

Abstract

Introduction

Conclusions

References

Tables

Figures

◀

▶

◀

▶

Back

Close

Full Screen / Esc

Printer-friendly Version

Interactive Discussion



Nakajima, T., Suzuki, K., and Stephens, G.: Droplet growth in warm water clouds observed by the A-Train. Part I: Sensitivity analysis of the MODIS-derived cloud droplet sizes, *J. Atmos. Sci.*, 67, 1884–1896, 2010a.

Nakajima, T., Suzuki, K., and Stephens, G.: Droplet growth in warm water clouds observed by the A-Train. Part II: A multisensor view, *J. Atmos. Sci.*, 67, 1897–1907, 2010b.

Painemal, D. and Zuidema, P.: Assessment of MODIS cloud effective radius and optical thickness retrievals over the Southeast Pacific with VOCALS-REx in situ measurements, *J. Geophys. Res.*, 116, D24, doi:10.1029/2011JD016155, 2011.

Penner, J. E., Xu, L., and Wang, M.: Satellite methods underestimate indirect climate forcing by aerosols, *P. Natl. Acad. Sci. USA*, 108, 13404–13408, 2011.

Platnick, S.: Vertical photon transport in cloud remote sensing problems, *J. Geophys. Res.*, 105, 22919–22935, 2000.

Pruppacher, H. R. and Lee, I.: A comparative study of the growth of cloud drops by condensation using an air parcel model with and without entrainment, *Pure Appl. Geophys.*, 115, 523–545, 1976.

Rao, V. D., Krishna, V. M., Sharma, K. V., and Rao, P. V. J. M.: Convective condensation of vapor in the presence of a non-condensable gas of high concentration in laminar flow in a vertical pipe, *Int. J. Heat Mass Tran.*, 51, 6090–6101, 2008.

Remer, L. A., Kleidman, R. G., Levy, R. C., Kaufman, Y. J., Tanré, D., Mattoo, S., Martins, J. V., Ichoku, C., Koren, I., Yu, H.-B., and Holben, B. N.: Global aerosol climatology from the MODIS satellite sensors, *J. Geophys. Res.*, 113, D14, doi:10.1029/2007jd009661, 2008.

Seinfeld, J. H. and Pandis, S. N.: *Atmospheric Chemistry and Physics*, John Wiley and Sons, New York, NY, 1998.

Platnick, S., King, M. D., Ackerman, S. A., Menzel, W. P., Baum, B. A., Riedi, J. C., and Frey, R. A.: The MODIS cloud products: algorithms and examples from Terra, *IEEE T. Geosci. Remote*, 41, 459–473, 2003.

Twomey, S.: The influence of pollution on the shortwave albedo of clouds, *J. Atmos. Sci.*, 34, 1149–1154, 1977.

Vignati, E., Facchini, M. C., Rinaldi, M., Scannell, C., Ceburnis, D., Sciare, J., Kanakidou, M., Myriokefalitakis, S., Dentener, F., and O’Dowd, C. D.: Global scale emission and distribution of sea-spray aerosol: sea-salt and organic enrichment, *Atmos. Environ.*, 44, 670–677, 2010.

Zeng, S.: Comparison and statistical analysis of cloud properties derived from POLDER and MODIS instruments into the framework of the A-Train spatial experiment, Ph. D. thesis, University Lille1, Villeneuve d'ascq, France, 2011.

5 Zhang, Z. and Platnick, S.: An assessment of differences between cloud effective particle radius retrievals for marine water clouds from three MODIS spectral bands, J. Geophys. Res., 116, D20, doi:10.1029/2011JD016216, 2011.

ACPD

13, 29035–29058, 2013

Global CDNC over ocean using A-Train satellites

S. Zeng et al.

Title Page

Abstract

Introduction

Conclusions

References

Tables

Figures

◀

▶

◀

▶

Back

Close

Full Screen / Esc

Printer-friendly Version

Interactive Discussion



Global CDNC over ocean using A-Train satellites

S. Zeng et al.

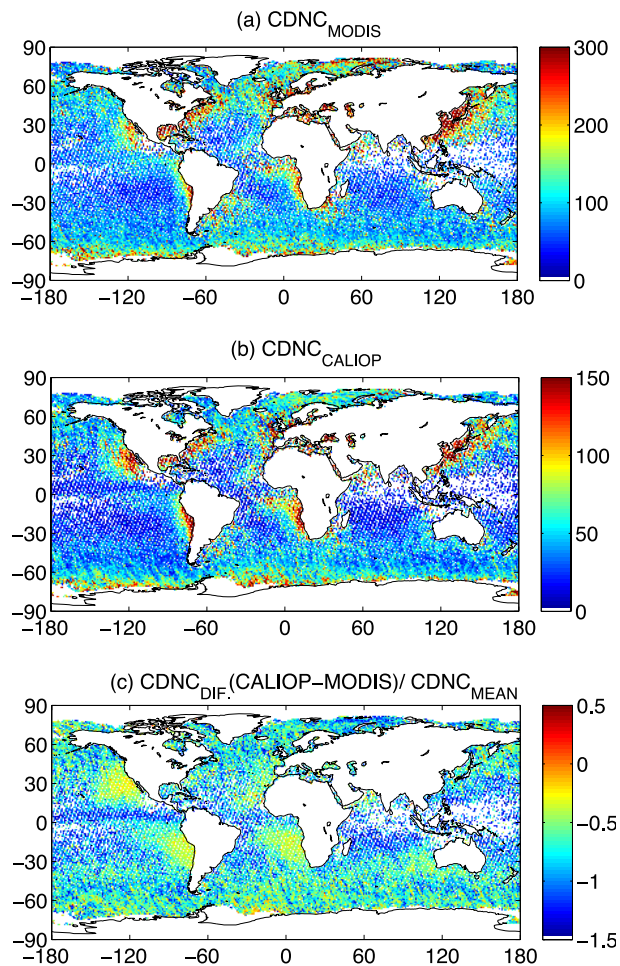


Fig. 1. Geographical distributions of CDNC derived from MODIS (a), CALIOP (b), and their relative differences (c). The MODIS 3.7 μm effective radius is used for the calculation.

Global CDNC over ocean using A-Train satellites

S. Zeng et al.

Title Page

Abstract

Introduction

Conclusions

References

Tables

Figures

◀

▶

◀

▶

Back

Close

Full Screen / Esc

Printer-friendly Version

Interactive Discussion

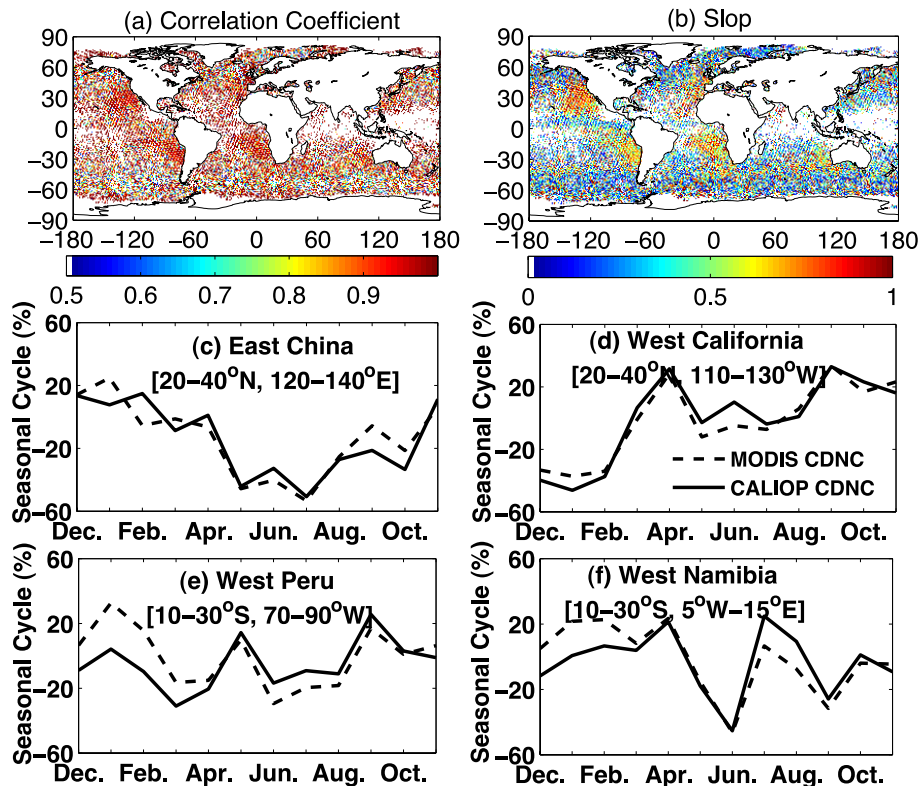


Fig. 2. Geographical distributions of the correlation coefficients **(a)** and the slopes **(b)** between monthly MODIS and CALIOP CDNCs, and seasonal variations of MODIS (dashed line) and CALIOP (solid line) CDNCs for four different regions: east of China **(c)**, regions of $20^{\circ}\text{N}\sim 40^{\circ}\text{N}$ and $120^{\circ}\text{E}\sim 140^{\circ}\text{E}$; west of California **(d)**, regions of $20^{\circ}\text{N}\sim 40^{\circ}\text{N}$ and $110^{\circ}\text{W}\sim 130^{\circ}\text{W}$; west of Peru **(e)**, regions of $10^{\circ}\text{S}\sim 30^{\circ}\text{S}$ and $70^{\circ}\text{W}\sim 90^{\circ}\text{W}$ and west of Namibia **(f)**, regions of $10^{\circ}\text{S}\sim 30^{\circ}\text{S}$ and $5^{\circ}\text{W}\sim 15^{\circ}\text{E}$.

Global CDNC over ocean using A-Train satellites

S. Zeng et al.

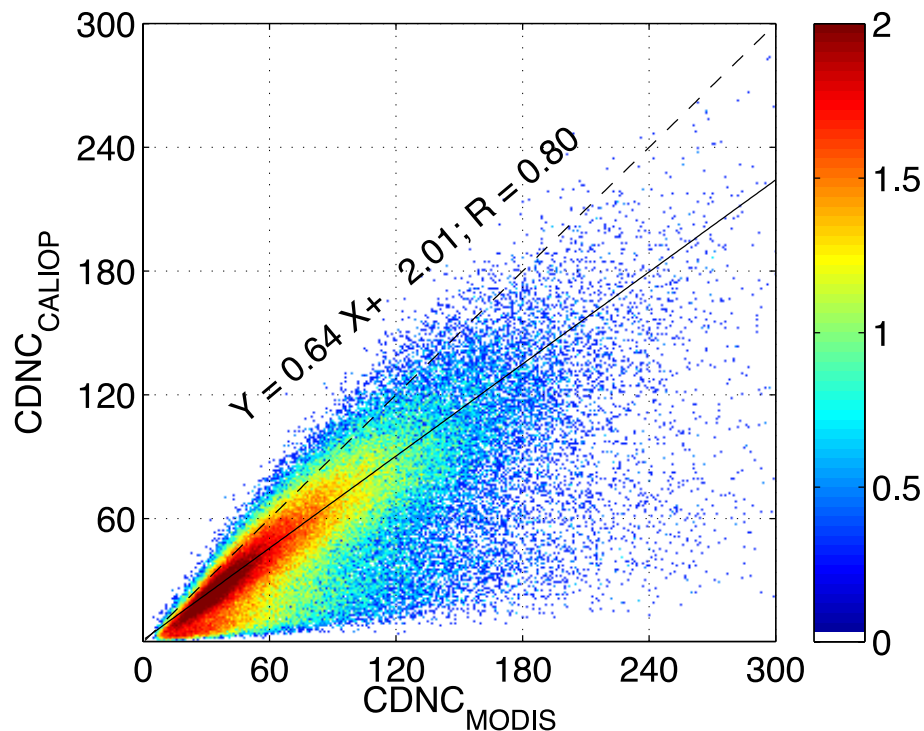


Fig. 3. Relationship between the MODIS and CALIOP CDNCs. The dashed line is the $x = y$ line, and the solid line is CDNC linear regression line. The color bar represents the logarithm of pixel number.

[Title Page](#)[Abstract](#)[Introduction](#)[Conclusions](#)[References](#)[Tables](#)[Figures](#)[◀](#)[▶](#)[◀](#)[▶](#)[Back](#)[Close](#)[Full Screen / Esc](#)[Printer-friendly Version](#)[Interactive Discussion](#)

Global CDNC over ocean using A-Train satellites

S. Zeng et al.

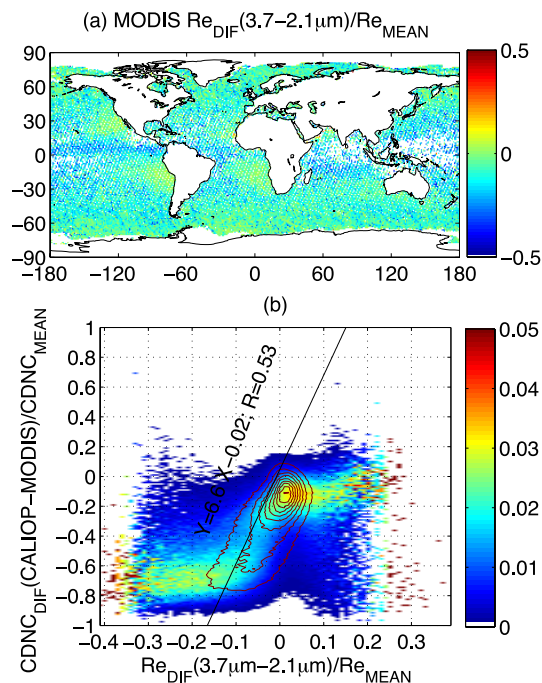


Fig. 4. Geographical distribution of relative difference of effective radius between 3.7 μm and 2.1 μm bands **(a)** and two dimensional histogram between relative CDNC differences and effective radius difference between 3.7 μm and 2.1 μm bands. The color bar represents normalized pixel number to each bin of effective radius difference. The solid straight line represents the linear relationship, and solid circle lines are isolines of pixel number.

[Title Page](#)
[Abstract](#)
[Introduction](#)
[Conclusions](#)
[References](#)
[Tables](#)
[Figures](#)
[◀](#)
[▶](#)
[◀](#)
[▶](#)
[Back](#)
[Close](#)
[Full Screen / Esc](#)
[Printer-friendly Version](#)
[Interactive Discussion](#)


Global CDNC over ocean using A-Train satellites

S. Zeng et al.

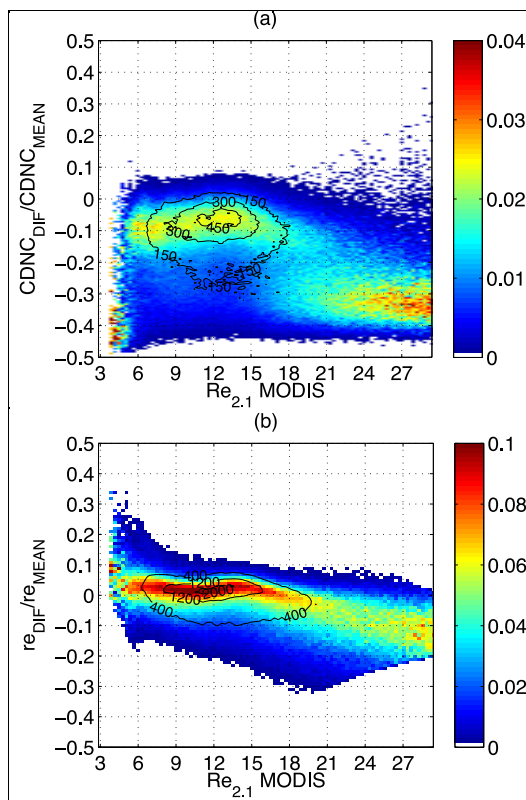


Fig. 5. Two dimensional histograms between relative CDNC differences and effective radius at $2.1 \mu\text{m}$ bands **(a)** and between relative effective radius differences and effective radius at $2.1 \mu\text{m}$ bands **(b)**. The color bar represents normalized pixel number to each effective radius bin. Solid circle lines are isolines of pixel number.

Global CDNC over ocean using A-Train satellites

S. Zeng et al.

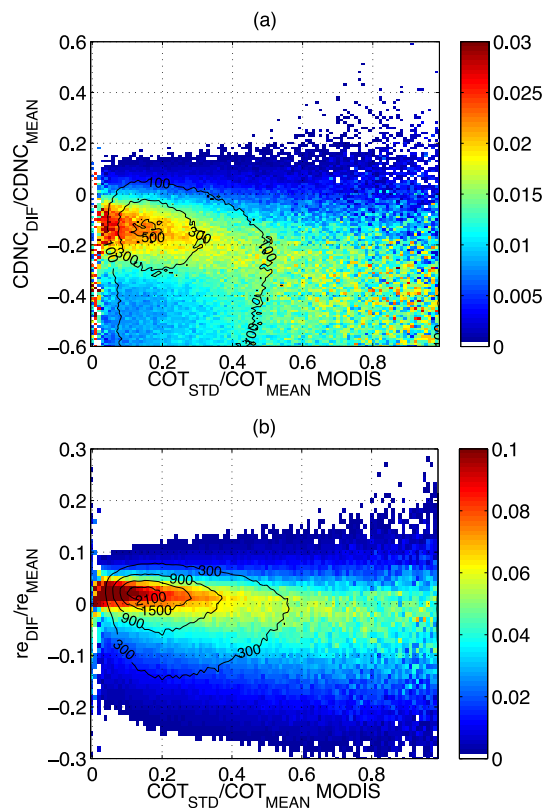


Fig. 6. Two dimensional histograms between relative CDNC differences and cloud heterogeneity **(a)** and between relative effective radius differences and cloud heterogeneity **(b)**. The color bar represents normalized pixel number to each effective radius bin. Solid circle lines are iso-lines of pixel number.

Global CDNC over ocean using A-Train satellites

S. Zeng et al.

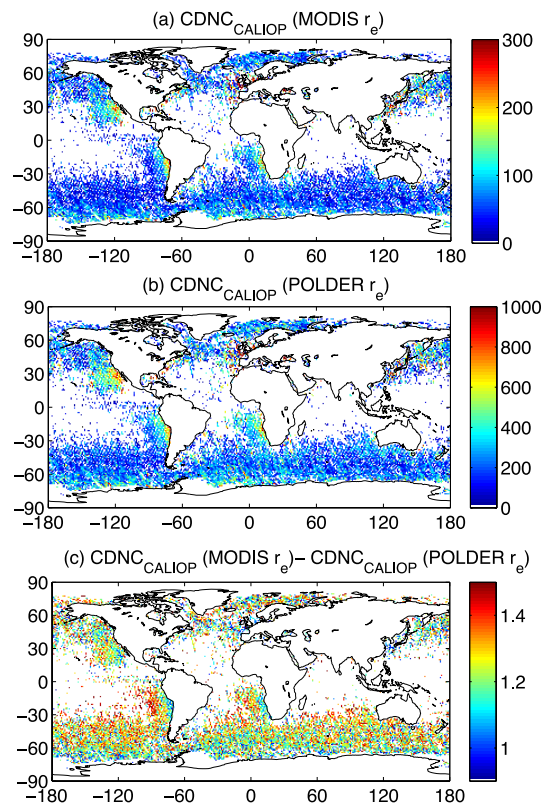


Fig. 7. Geographic distributions of CALIOP CDNC derived using MODIS $r_{e,3.7}$ (a), POLDER r_e (b), and relative differences between them.